

Thiosulfate- and Thiosulfonate-Based Etchants for the Patterning of Gold Using Microcontact Printing

Dirk Burdinski* and Martin H. Blees†

Bio-Molecular Engineering, Philips Research Europe, High Tech Campus 11,
5656 AE Eindhoven, The Netherlands

Received March 28, 2007. Revised Manuscript Received May 31, 2007

The transcription of microcontact-printed self-assembled monolayer patterns into gold substrates requires a wet chemical etch process that selectively dissolves unprotected metal without attacking SAM-covered gold regions. Gold dissolution in a standard thiosulfate–ferricyanide etch solution, the most commonly used etchant containing sulfur-based ligands, shows a complex kinetic behavior. Etch-rate-determining under most conditions are the concentrations of thiosulfate, ferricyanide, and hydroxide. The etch process is accelerated under high ionic strength conditions, in particular in the presence of potassium ions. This is ascribed to the formation of potassium–reagent ion pairs, which reduce the Coulomb repulsion between the negatively charged reaction partners. The thiosulfate–ferricyanide etchant is intrinsically unstable due to the reduction of the ferricyanide oxidant during thiosulfate decomposition. The gold ligand thiosulfate was therefore substituted with benzenethiosulfonate, which was expected to be less oxidation sensitive. The new bath decomposed in the course of days instead of several hours. Since the etch efficiency was also reduced, a significantly higher concentration of the gold ligand was required to achieve a sufficiently high etch rate. The somewhat lower etch quality of the new bath could be compensated for by introducing a new defect healing additive, 1-decanesulfonamide, which was found to be more effective than 1-octanol in the new etchant.

Introduction

Surface patterning on the micron and submicron scale is gaining increasing importance. A common aspect of emerging biomedical and electronic device technologies is the need for cheap, simple, and highly flexible surface structuring techniques. Against this background, microcontact printing (μ CP), as well as other soft-lithographic micropatterning techniques, have undergone a remarkable development over the past decade, due to their simplicity and general compatibility with biosensor devices, including the patterned deposition of functional proteins or polynucleotide markers.^{1–4}

μ CP enables the local modification of typically metal surfaces with patterned self-assembled monolayers (SAMs) of amphiphatic, organic molecules. SAMs are deposited selectively in the areas of contact by printing with an elastomeric stamp that bears the desired surface relief structure and that is loaded with an appropriate ink solution. Due to their generally high stability, SAMs can be employed as a resist to transcribe the pattern into the underlying metal layers by etching, as a template for further selective material deposition, or to achieve a surface functionalization for

another purpose.^{5,6} Typical substrate materials are Au, Ag, Cu, Pd, Si, and Al. Gold in particular has proven to be most suitable for the surface immobilization of biological molecules, due to its chemical inertness and biocompatibility as well as the ease of SAM formation on its surface utilizing alkanethiol derivatives. Gold is also a preferred electrode metal in organic semiconductor devices. The microcontact patterning of gold surfaces is therefore of utmost academic and industrial importance.

The transcription of printed SAM patterns into a gold surface requires a wet chemical etch process that selectively dissolves unprotected gold without attacking SAM-covered metal. Etch solutions that have proven to be useful in combination with patterned SAM resists are different from those classically used in the electronics industry. This is mainly due to the lower etch stability of SAMs, which are only a few nanometers thick, as compared to conventional photoresists, which are applied in an up to micrometer thickness.

The two fundamental components of a gold etchant are a ligand that binds the oxidized metal ion, thereby decreasing its redox potential, and a sufficiently strong oxidant to achieve gold oxidation in the presence of this ligand.^{7–9} Obviously both components must not disrupt the integrity

* Corresponding author. E-mail: dirk.burdinski@philips.com.

† Current Address: Central Development Lighting, Philips Lighting, Mathildelaan 1, 5611 BD Eindhoven, The Netherlands.

- (1) Menard, E.; Rogers, J. A. In *Springer Handbook of Nanotechnology*, 2nd ed.; Bhushan, B., Ed.; Springer: New York, 2007; pp 279–297.
- (2) Rogers, J. A.; Nuzzo, R. G. *Mater. Today* **2005**, *8*, 50–56.
- (3) Gates, B. D.; Xu, Q.; Stewart, M.; Ryan, D.; Willson, C. G.; Whitesides, G. M. *Chem. Rev.* **2005**, *105*, 1171–1196.
- (4) Quist, A. P.; Pavlovic, E.; Oscarsson, S. *Anal. Bioanal. Chem.* **2005**, *381*, 591–600.

- (5) Love, J. C.; Estroff, L. A.; Kriebel, J. K.; Nuzzo, R. G.; Whitesides, G. M. *Chem. Rev.* **2005**, *105*, 1103–1169.
- (6) Onclin, S.; Ravoo, B. J.; Reinhoudt, D. N. *Angew. Chem. Int. Ed.* **2005**, *44*, 6282–6304.
- (7) Nicol, M. J. *Gold Bull.* **1980**, *13*, 46–55.
- (8) Nicol, M. J. *Gold Bull.* **1980**, *13*, 105–111.
- (9) Senanayake, G. *Miner. Eng.* **2004**, *17*, 785–801.

of the SAM resist. In a conventional iodine–iodide etchant, iodine is used as the oxidant to dissolve gold as an iodide complex.¹⁰ This etchant was, however, found to be too aggressive against alkanethiol SAM resists, causing a large number of etch defects.¹¹ Ligands that reduce the gold redox potential even more, in particular thiourea, thiosulfate, and cyanide, have proven to be more suitable.^{11,12} Thiourea-based etchants were described to provide a poor edge resolution with hydrogen peroxide as the oxidant and a pure alkanethiol etch resist.¹³ They have nevertheless been applied successfully in combination with simple ferric salts as the oxidant^{14,15} and have proven to be particularly useful in positive printing schemes, in which the penetration of a dedicated SAM is even desired.^{16–18} The charge neutrality of the molecule, which allows it to penetrate hydrophobic SAM layers more easily compared to charged molecules, is assumed to be a key aspect resulting in a poorer SAM stability.¹⁷ Cyanide and thiosulfate are the most frequently used etch-promoting ligands. In the case of cyanide even air oxygen can be utilized as the oxidant.^{19–21} The most popular oxidant in combination with these two ligands, however, is the ferricyanide anion, in part because its oxidation power can in practice be controlled easily, for instance, by the addition of a ferrocyanide salt.^{11,13}

There are a number of important shortcomings of the above etch baths. The use of cyanide is highly undesirable, particularly in an industrial setting, due to its high toxicity and the risk of HCN gas formation.^{11,13} Thiourea, which is also considered a potential carcinogen, and thiosulfate, on the other hand, are oxidation sensitive, and oxidation of the ligand is thermodynamically even favored over gold oxidation.^{7,22} Hence, etchants containing these ligands are chemically metastable and decompose due to oxidative degradation of the ligand by the oxidizing agent. A new etchant based on mercaptoethylamine as the ligand in ammoniacal ethanol solution, supposedly using air oxygen as the oxidant, has recently been proposed, but the stability of the bath has not been reported.²³

The implementation of μ CP in industrial processes, therefore, critically depends on the development of novel gold etch solutions with an improved durability. In this paper, we describe a first approach toward such an improved etchant. The impact of the different reagents of a standard thiosulfate–ferricyanide etchant on the gold etch performance was analyzed. On this basis, new etch solutions were tested, in which thiosulfate ($S_2O_3^{2-}$) is substituted with benzenethiosulfonate ($PhS_2O_2^-$). We speculated that the smaller negative charge of this compound compared to thiosulfate would make it less sensitive to oxidative decomposition. The stability and the etch performance of both etchants are compared.

Materials and Methods

Materials. Lithium hydroxide hydrate (56% LiOH), sodium perchlorate (pure), and sodium decanesulfonate (NaDS, 96%) were purchased from ACROS. Ethanol, *n*-heptane, potassium hydroxide, and sodium hydroxide (all p.a. grade) were received from Merck. *n*-Octadecanethiol (ODT, 98% purity), potassium thiosulfate monohydrate (99%), sodium thiosulfate (99%), potassium ferricyanide (99%), potassium ferrocyanide (99%), sodium benzenethiosulfonate (85%, techn), and *n*-octanol (99%) were purchased from Aldrich. 1-Decanesulfonamide was purchased from LaboTest, Germany. All chemicals were used as received. All etch solutions were prepared using deionized water.

The stamp material, Sylgard-184 polydimethylsiloxane (PDMS), was obtained from Dow Corning. It was mixed in a 1:10 curing agent/prepolymer ratio, cured overnight at 65 °C, and postcured at room temperature for at least 1 month. Silicon wafers were modified with an about 500 nm thick thermal silicon oxide layer, a titanium adhesion layer (5 nm, evaporated) on top, and finally with an evaporated gold layer with a thickness of typically 25 nm, unless indicated otherwise. Prior to use, the substrates with a size of 5 × 5 mm² (for unpatterned use) or 10 × 20 mm² (for patterning experiments) were rinsed with, subsequently, ultrapure water (resistivity > 18 MΩ·cm), ethanol, and heptane. They were thereafter exposed to a TEPLA 300E microwave argon plasma (0.25 mbar Ar, 300 W, 5 min).

Unless indicated otherwise, the etch solutions were prepared from two or three aqueous stock solutions just before the actual etch experiment. Typically, one stock solution contained the ligand in a basic milieu and a second stock solution contained the oxidant in a pH neutral milieu. Depending on the parameter that was varied, a third stock solution may have been used (e.g., when varying the ionic strength of the medium). The total volume of the final etch solutions for each individual etch experiment was 20 mL. Final mixed etch solutions were used only once.

Microcontact Printing. PDMS stamps (about 10 × 20 mm²) bearing various electronic test patterns were equilibrated for a minimum of 2 h in an ethanolic ODT ink solution (2 mM). After removal from the ink solutions, the stamps were rinsed briefly with ethanol and dried in a stream of nitrogen for about 30 s immediately prior to use. Stamping was performed manually by using tweezers for stamp handling and by taking advantage of the natural stamp–substrate adhesion. No extra pressure was applied.

Etching. Etching was performed under moderate stirring with a magnetic stir bar in open polyethylene containers generally without special precautions with respect to air or light exposure. In temperature-variation studies, etching was performed in reaction vessels with a temperature-controlled jacket (± 0.2 °C). Samples were immersed in the etch solutions and the required etch time for

- (10) Eidelloth, W.; Sandstrom, R. L. *Appl. Phys. Lett.* **1991**, *59*, 1632–1634.
- (11) Kumar, A.; Biebuyck, H. A.; Whitesides, G. M. *Langmuir* **1994**, *10*, 1498–1511.
- (12) Xia, Y.; Zhao, X.-M.; Whitesides, G. M. *Microelectron. Eng.* **1996**, *32*, 255–268.
- (13) Xia, Y.; Zhao, X.-M.; Kim, E.; Whitesides, G. M. *Chem. Mater.* **1995**, *7*, 2332–2337.
- (14) Balmer, T. E.; Schmid, H.; Stutz, R.; Delamarche, E.; Michel, B.; Spencer, N. D.; Wolf, H. *Langmuir* **2005**, *21*, 622–632.
- (15) Geissler, M.; Wolf, H.; Stutz, R.; Delamarche, E.; Grummt, U.-W.; Michel, B.; Bietsch, A. *Langmuir* **2003**, *19*, 6301–6311.
- (16) Delamarche, E.; Geissler, M.; Wolf, H.; Michel, B. *J. Am. Chem. Soc.* **2002**, *124*, 3834–3835.
- (17) Saalmink, M.; van der Marel, C.; Stapert, H. R.; Burdinski, D. *Langmuir* **2006**, *22*, 1016–1026.
- (18) Perl, A.; Péter, M.; Ravoo, B. J.; Reinhoudt, D. N.; Huskens, J. *Langmuir* **2006**, *22*, 7568–7573.
- (19) Kumar, A.; Biebuyck, H. A.; Abbott, N. L.; Whitesides, G. M. *J. Am. Chem. Soc.* **1992**, *114*, 9188–9189.
- (20) Kumar, A.; Whitesides, G. M. *Appl. Phys. Lett.* **1993**, *63*, 2002–2004.
- (21) Wilbur, J. L.; Kumar, A.; Kim, E.; Whitesides, G. M. *Adv. Mater.* **1994**, *6*, 600–604.
- (22) Hiskey, J. B.; Atluri, V. P. *Miner. Process. Extra. Metall. Rev.* **1988**, *4*, 95–134.
- (23) Ducker, R. E.; Leggett, G. J. *J. Am. Chem. Soc.* **2006**, *128*, 392–393.

removal of the complete gold layer (time to clear, TTC) was determined by optical inspection. The end of the etch process was reached when the dark-greenish-purple color of the underlying titanium/silicon oxide layer was clearly visible over the entire surface area. The etch process was stopped by quickly removing the substrate from the etch solution and washing it with a large volume of distilled water at room temperature. To determine very accurate etch rates and the activation energy of the etch process from temperature-variation studies, the etch reaction was stopped in some cases prior to completion after certain time intervals, and the remaining layer thickness was determined by Rutherford backscattering (RBS) analysis. In all other experiments, average etch rates were calculated as $v = d/\text{TTC}$ assuming a linear etch process for the $d = 25$ nm thick gold films. All experiments (except RBS studies) were done in duplicate.

Decomposition Studies. Freshly prepared stock solutions of the bath components were mixed at time point zero of each experiment. UV/vis spectra were recorded with a Lambda 900 UV/vis/NIR spectrometer (Perkin-Elmer) and quartz cuvettes (path length 10 mm, volume about 3 mL). At different time points aliquots of the etch solutions (0.3 mL) were diluted with deionized water (2.7 mL) to record each spectrum. Baseline spectra were recorded with deionized water in the same cuvette. In parallel, etch experiments were performed using the same etch solutions.

Elemental Analysis. The concentration of 1-decanesulfonamide (DSA) in saturated solutions in water and in a 1.0 M aqueous solution of potassium hydroxide was determined by inductively coupled plasma atomic emission spectrometry (ICP-AES) on a Jobin Yvon JY 38 plus spectrometer using the sulfur emission maximum at 181.978 nm. The given range of the experimental error indicates three times the difference between experimental (c_{exp}) and average concentration values (c_{avg}) of two independent experiments.

Surface Analysis. Optical micrographs were taken of etched patterns. Atomic force microscopy (AFM) was performed on a Veeco MultiMode scanning probe microscope with a NanoScope IV controller or on a TopoMetrix Accurex II system in noncontact (tapping) mode using an Ultrasharp μ Mash NSC16 type A cantilever. RBS experiments were carried out with a High Voltage Engineering 2.5 MeV-v.d.Graaff accelerator using a monochromatic beam of 2 MeV $^4\text{He}^+$ ions and a home-built beam line and electronics setup. The energy of the backscattered He^+ ions was analyzed with the aid of a surface-barrier detector using backscattering angles of 170° and 100° . Spectra were simulated using the RUMP program package.

Results

Thiosulfate-Based Etchants. Thiosulfate-based etchants are currently most frequently used for the selective etching of SAM-modified gold surfaces; hence, such etchants were the starting point of this study. The gold layer was dissolved from unpatterned gold substrates (23 nm Au) by etching with a standard thiosulfate–ferricyanide etch bath ($[\text{KOH}] = 1.0$ M, $[\text{K}_2\text{S}_2\text{O}_3] = 0.1$ M, $[\text{K}_3\text{Fe}(\text{CN})_6] = 0.01$ M, $[\text{K}_4\text{Fe}(\text{CN})_6] = 0.001$ M).¹³ The etch reaction was quenched after different time intervals and the thickness of the remaining gold layer was determined by RBS analysis. The results obtained at four different temperatures between 5 and 35°C are summarized in Figure 1A, in which the thickness of the remaining gold layer is plotted against the respective etch time.

At all studied temperatures a linear decrease of the remaining gold thickness over time was found yielding etch

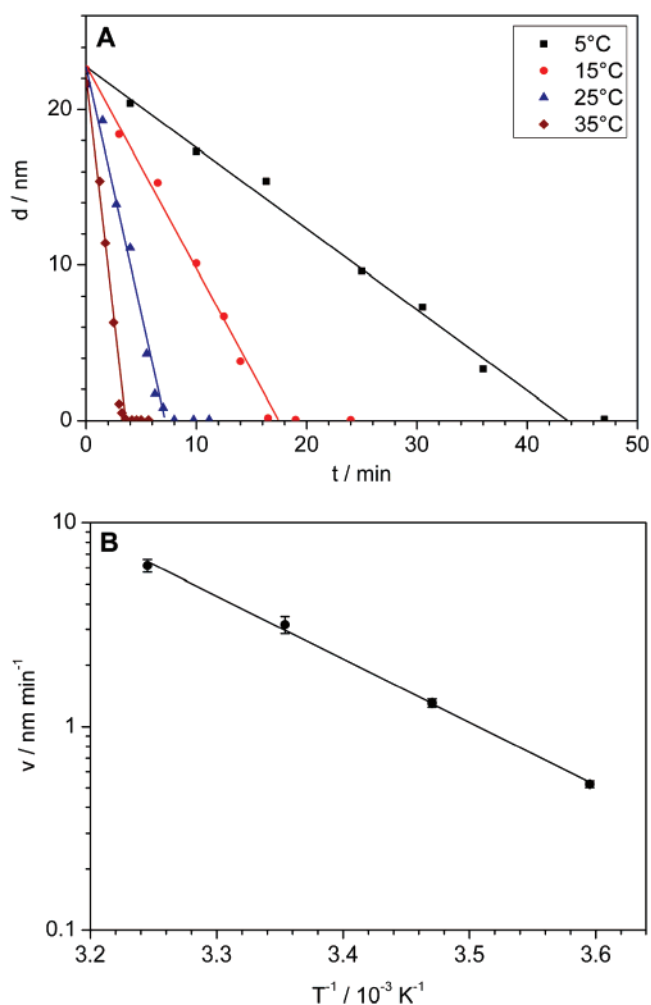


Figure 1. The thickness of the remaining gold layer as determined by RBS analysis after etching of gold substrates with a standard thiosulfate–ferricyanide etch bath ($[\text{KOH}] = 1.0$ M, $[\text{K}_2\text{S}_2\text{O}_3] = 0.1$ M, $[\text{K}_3\text{Fe}(\text{CN})_6] = 0.01$ M, $[\text{K}_4\text{Fe}(\text{CN})_6] = 0.001$ M) as a function of the etch time at four different temperatures (A). Linear regression analysis yielded average etch rates of $0.52 \pm 0.02 \text{ nm} \cdot \text{min}^{-1}$ (5°C , $R = 0.996$), $1.31 \pm 0.06 \text{ nm} \cdot \text{min}^{-1}$ (15°C , $R = 0.990$), $3.17 \pm 0.31 \text{ nm} \cdot \text{min}^{-1}$ (25°C , $R = 0.995$), and $6.16 \pm 0.45 \text{ nm} \cdot \text{min}^{-1}$ (35°C , $R = 0.999$). Plot of these etch rates as a function of temperature (B). Linear regression analysis yielded an activation energy of $E_a = 59 \pm 2 \text{ kJ} \cdot \text{mol}^{-1}$.

rates between about 0.5 and $6.2 \text{ nm} \cdot \text{min}^{-1}$ at 5 and 35°C , respectively. On this basis, in all later experiments a linear etch progress was assumed to calculate average etch rates from observed total etch times for gold layers of a known thickness. The above etch rates were plotted in an Arrhenius type plot of $\log(v)$ vs $1/T$ (Figure 1B), from which the activation energy of the etching reaction was determined to be $59 \pm 2 \text{ kJ} \cdot \text{mol}^{-1}$.

To study the influence of the various bath components on the reaction kinetics, in a first set of experiments gold substrates were etched with thiosulfate–ferricyanide etch baths containing various concentrations of $\text{S}_2\text{O}_3^{2-}$ with an accordingly changing or a constant ($\mu = 4.0$ M) ionic strength. The observed etch rates (blue squares and red circles) are plotted in Figure 2 as a function of the thiosulfate concentration. A linear dependence of the etch rate on $\log[\text{S}_2\text{O}_3^{2-}]$ was observed. The same dependence was found for earlier published data after recalculating etch rates from reported etch times assuming a linear etch process (green triangles).

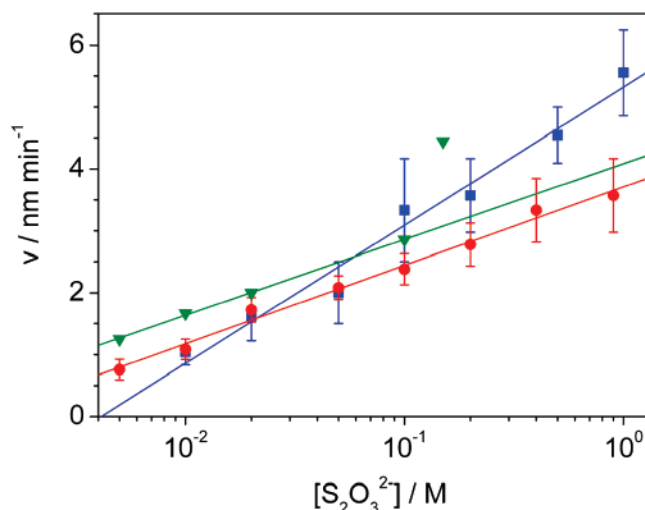


Figure 2. Average etch rate for 25 nm gold layers as a function of $[S_2O_3^{2-}]$ in the following etchants: $[base] = 1.0$ M (KOH or NaOH), $[K_3Fe(CN)_6] = 0.01$ M, $[K_4Fe(CN)_6] = 0.001$ M, μ = variable or 4.0 M (NaClO₄) (linear regression, 1 σ values). Blue squares: KOH, μ = variable [$v = 5.3(2)$ nm·min⁻¹ + 2.2(2) nm·min⁻¹ × log $[S_2O_3^{2-}]/M$ ($R = 0.988$)]; red circles: NaOH, $\mu = 4.0$ M [$v = 3.71(7)$ nm·min⁻¹ + 1.27(5) nm·min⁻¹ × log $[S_2O_3^{2-}]/M$ ($R = 0.996$)]; green triangles: KOH, μ = variable [$v = 4.09$ nm·min⁻¹ + 1.22 nm·min⁻¹ × log $[S_2O_3^{2-}]/M$ (data from Xia et al.¹³ calculated for 20 nm gold films, data point at highest concentration omitted for linear regression)].

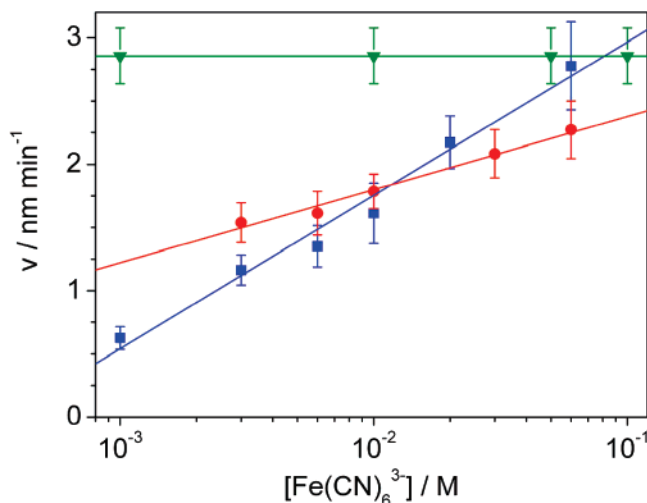


Figure 3. Average etch rate for 25 nm gold layers as a function of $[Fe(CN)_6^{3-}]$ in the following etchants: $[base] = 1.0$ M (KOH or NaOH), $[Na_2S_2O_3] = 0.1$ M, $[K_4Fe(CN)_6] = 0.1 \times [K_3Fe(CN)_6]$, μ = variable or 4.0 M (NaClO₄) (linear regression, 1 σ values). Blue squares: NaOH, μ = variable [$v = 4.2(2)$ nm·min⁻¹ + 1.2(1) nm·min⁻¹ × log $[S_2O_3^{2-}]/M$ ($R = 0.990$)]; red circles: NaOH, $\mu = 4.0$ M [$v = 3.0(1)$ nm·min⁻¹ + 0.58(5) nm·min⁻¹ × log $[S_2O_3^{2-}]/M$ ($R = 0.993$)]; green triangles: KOH, μ = variable ($v = 2.86$ nm·min⁻¹, data from Xia et al.¹³ calculated for 20 nm gold films).

Figure 3 summarizes the results obtained in a second set of experiments, in which respective etch solutions containing a constant thiosulfate concentration, but different concentrations of the ferricyanide–ferrocyanide redox couple, were used (red circles and blue squares). In contrast to the data reported by Xia et al. (green triangles), who observed no dependence on the ferricyanide concentration, we found the etch rate to depend linearly on log $[Fe(CN)_6^{3-}]$, irrespective of the ionic strength being maintained at a constant value or not. All etch rates, nevertheless, converge at a $[Fe(CN)_6^{3-}]$ of about 0.1 M. These data do not permit us to conclude there is a strong influence of the ionic strength on the etch

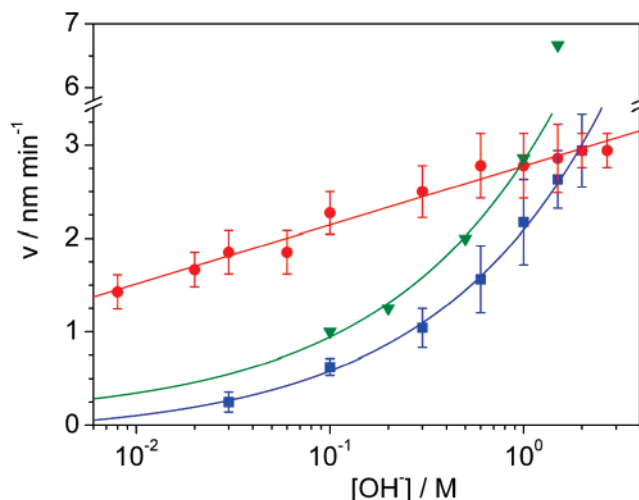


Figure 4. Average etch rate for 25 nm gold layers as a function of $[OH^-]$ (KOH or NaOH) in the following etchants: $[Na_2S_2O_3] = 0.1$ M, $[K_3Fe(CN)_6] = 0.01$ M, $[K_4Fe(CN)_6] = 0.001$ M, μ = variable or 4.0 M (NaClO₄) (linear regression, 1 σ values). Blue squares: KOH, μ = variable [$v = 0.12(5)$ nm·min⁻¹ + 2.21(6) nm·min⁻¹ × ($[OH^-]/M$)^{1/2} ($R = 0.999$)]; red circles: NaOH, $\mu = 4.0$ M [$v = 2.77(4)$ nm·min⁻¹ + 0.63(4) nm·min⁻¹ × log($[OH^-]/M$) ($R = 0.990$)]; green triangles: KOH, μ = variable ($v = 0.1$ nm·min⁻¹ + 2.8 nm·min⁻¹ × ($[OH^-]/M$)^{1/2}, data from Xia et al.¹³ calculated for 20 nm gold films, data point at highest concentration omitted).

rate, since the overall change of the ionic strength in this experiment was small.

It is known that the gold etch rate with thiosulfate-based baths increases with an increase in pH. In most cases, strongly alkaline thiosulfate solutions are therefore used, also because a high pH is important to prevent fast decomposition of these solutions. We varied the pH in the range between about 7 and 14, in which the stability of the etch bath was sufficiently high to perform etch experiments, both at constant and at variable ionic strength, without significant self-decomposition of the bath in the experimental time frame (Figure 4).

Comparing the etch rates at variable ionic strength, we obtained somewhat smaller rates (blue squares) than Xia et al. (green triangles). Despite this small difference, both data sets could be fitted consistently with a $v \sim [OH^-]^{1/2}$ model; a very good fit could only be obtained disregarding the data point at the highest reported concentration (green triangles). A linear etch rate dependence on log $[OH^-]$ was, however, found in the experiments performed at a constant ionic strength (red circles). This indicates that the linear dependence on $[OH^-]^{1/2}$ observed in the other subset of experiments reflects the combined effect of a logarithmic dependence on the hydroxide concentration and an unknown dependence on the ionic strength of the etch medium and on the type of counter cation, which was different for the two experiments.

A general influence of the ionic strength μ of the etch solution on the etch rate has been observed in the preceding experiments. Therefore, an experiment was performed under systematic variation of this parameter by adding various amounts of sodium perchlorate, which was assumed to be not directly involved in the etch reaction, to the bath (Figure 5). The etch rate increased linearly with log $[\mu]$, which indicates that, in the rate-determining step of the overall etch reaction, species with the same (partial) charge have to

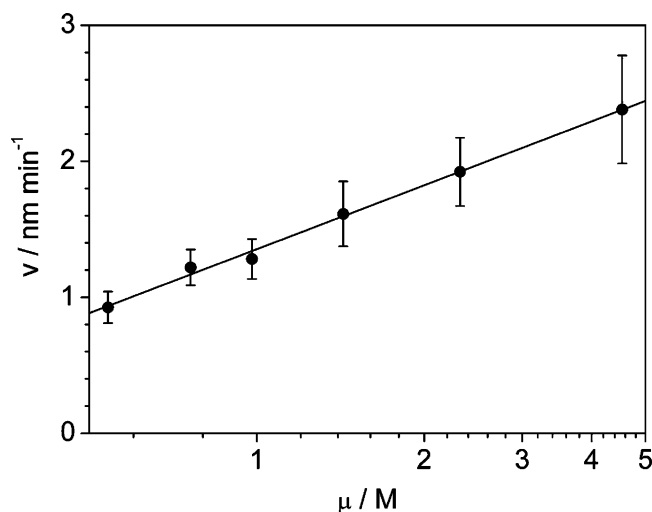


Figure 5. Average etch rate for 25 nm gold layers as a function of the total ionic strength μ (adjusted by NaClO_4 addition) in the following etchant: $[\text{NaOH}] = 1.0 \text{ M}$, $[\text{Na}_2\text{S}_2\text{O}_3] = 0.1 \text{ M}$, $[\text{K}_3\text{Fe}(\text{CN})_6] = 0.01 \text{ M}$, $[\text{K}_4\text{Fe}(\text{CN})_6] = 0.001 \text{ M}$. Linear regression (1σ values): $v = 0.35(2) \text{ nm}\cdot\text{min}^{-1} + 1.56(5) \text{ nm}\cdot\text{min}^{-1} \times \log(\mu/\text{M})$ ($R = 0.998$).

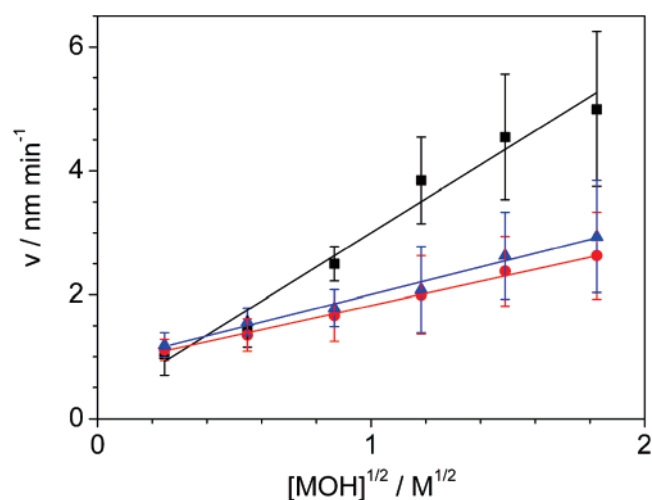


Figure 6. Average etch rate for 25 nm gold layers as a function of $[\text{MOH}]^{1/2}$ ($\text{M} = \text{Li, Na, K}$) in the following etchant: $[\text{K}_2\text{S}_2\text{O}_3] = 0.1 \text{ M}$, $[\text{K}_3\text{Fe}(\text{CN})_6] = 0.01 \text{ M}$, $[\text{K}_4\text{Fe}(\text{CN})_6] = 0.001 \text{ M}$, $\mu = \text{variable}$ (linear regression, 1σ values). Black squares: KOH [$v = 0.3(3) \text{ nm}\cdot\text{min}^{-1} + 2.8(3) \text{ nm}\cdot\text{min}^{-1} \times ([\text{OH}^-]/\text{M})^{1/2}$ ($R = 0.98$)]]; red circles: NaOH [$v = 0.86(3) \text{ nm}\cdot\text{min}^{-1} + 0.97(4) \text{ nm}\cdot\text{min}^{-1} \times ([\text{OH}^-]/\text{M})^{1/2}$ ($R = 0.997$)]]; blue triangles: LiOH [$v = 0.89(8) \text{ nm}\cdot\text{min}^{-1} + 1.11(7) \text{ nm}\cdot\text{min}^{-1} \times ([\text{OH}^-]/\text{M})^{1/2}$ ($R = 0.993$)]].

approach each other.⁸ It is reasonable to assume that in the strongly basic medium (1.0 M NaOH) this reflects the reaction between the negatively charged components of the bath ($\text{S}_2\text{O}_3^{2-}$, $\text{Fe}(\text{CN})_6^{3-}$) and the gold surface, which is partially oxidized bearing either oxide or thiosulfate ligands, both imposing negative surface charges.

The above experiments also point to an influence of the counter cation on the etch rate. We therefore studied this effect in an etch experiment using the three bases lithium, sodium, and potassium hydroxide at variable concentrations and variable ionic strength (Figure 6). Under these conditions, a linear dependence of the etch rate on the square root of the potassium hydroxide concentration was described above and here also confirmed for the other two alkali hydroxides. The differences in etch rate between lithium and sodium hydroxide were not significant, but both etch rates were significantly lower than that found for potassium hydroxide,

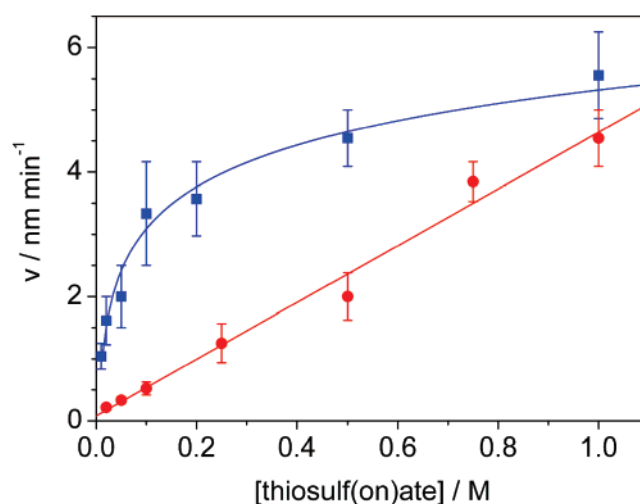


Figure 7. Average etch rate for 25 nm gold layers as a function of $[\text{PhS}_2\text{O}_2^-]$ and $[\text{S}_2\text{O}_3^{2-}]$ in the following etchant: $[\text{KOH}] = 1.0 \text{ M}$, $[\text{K}_3\text{Fe}(\text{CN})_6] = 0.01 \text{ M}$, $[\text{Na}_2\text{S}_2\text{O}_3] = 0.1 \text{ M}$, $[\text{K}_4\text{Fe}(\text{CN})_6] = 0.001 \text{ M}$, $\mu = \text{variable}$ (data fitting function, 1σ values). Blue squares: $\text{S}_2\text{O}_3^{2-}$ [$v = 5.3(2) \text{ nm}\cdot\text{min}^{-1} + 2.2(2) \text{ nm}\cdot\text{min}^{-1} \times \log([\text{S}_2\text{O}_3^{2-}]/\text{M})$ ($R = 0.988$), replotted from Figure 2]; red circles: PhS_2O_2^- [$v = 0.1(2) \text{ nm}\cdot\text{min}^{-1} + 4.6(3) \text{ nm}\cdot\text{min}^{-1} \times [\text{PhS}_2\text{O}_2^-]/\text{M}$ ($R = 0.993$)]].

which makes potassium hydroxide the base of choice for achieving a high overall etch rate.

Comparison of Thiosulfate- and Benzenethiosulfonate-Based Etchants. Despite their excellent etch performance, thiosulfate-based etch baths suffer from self-decomposition, which makes them useful for only short time intervals ranging from some 30 min to a few hours, depending on their exact composition. As part of this study, therefore, alternative etch baths were considered, in which thiosulfate is substituted with benzenethiosulfonate. We speculated that the lower negative charge of the monoanionic aromatic sulfonate compared to dianionic thiosulfate would make it less sensitive to oxidative decomposition. First, the gold dissolution performance of both etchants is compared, before decomposition studies are reported.

Similar to the above-described experiments with the thiosulfate etchant, gold substrates were etched with benzenethiosulfonate–ferricyanide etch baths containing different concentrations of PhS_2O_2^- . The observed etch rates (red circles) are plotted in Figure 7 as a function of the benzenethiosulfonate concentration. A linear dependence of the etch rate on $[\text{PhS}_2\text{O}_2^-]$ was found, which is quite different from the above-reported linear increase of the etch rate with $\log[\text{S}_2\text{O}_3^{2-}]$ in the case of the thiosulfate bath (blue squares). Particularly at low ligand concentrations, etch rates were significantly higher for the thiosulfate bath at any ligand concentration below about 1 M, at which concentration the etch rate difference between the two baths became insignificant. In the intermediate ligand concentration range, similar etch rates of about $2.5 \text{ nm}\cdot\text{min}^{-1}$ can be expected for solutions containing $[\text{S}_2\text{O}_3^{2-}] = 0.05 \text{ M}$ and those containing $[\text{PhS}_2\text{O}_2^-] = 0.5 \text{ M}$ with identical concentrations of the other bath components. These two baths were therefore selected for the below described decomposition study.

Whereas the etch rate of the thiosulfate bath was found to depend linearly on $\log[\text{Fe}(\text{CN})_6^{3-}]$ up to molar concentrations (Figure 3), in the case of benzenethiosulfonate such a linear

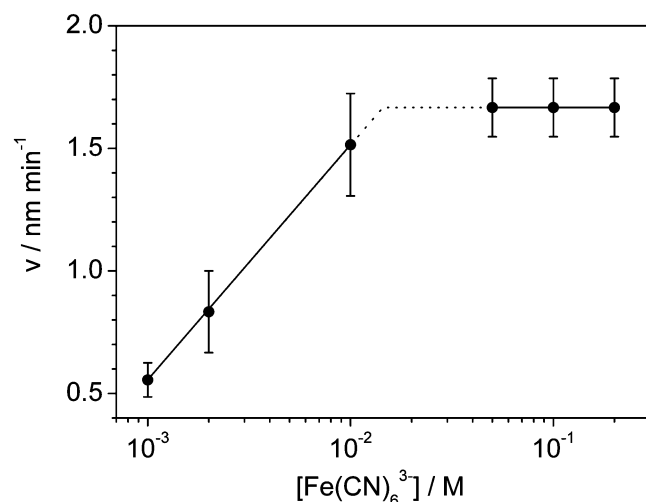


Figure 8. Average etch rate for 25 nm gold layers as a function of $[\text{Fe}(\text{CN})_6^{3-}]$ in the following etchant: $[\text{KOH}] = 1.0 \text{ M}$, $[\text{Na}(\text{PhS}_2\text{O}_2)] = 0.5 \text{ M}$, $[\text{K}_4\text{Fe}(\text{CN})_6] = 0.1 \times [\text{K}_3\text{Fe}(\text{CN})_6]$, $\mu = \text{variable}$ (linear regression, 1σ values). For $[\text{Fe}(\text{CN})_6^{3-}] = 10^{-2}$ – 10^{-3} M : $v = 3.43(4) \text{ nm}\cdot\text{min}^{-1} - 0.96(2) \text{ nm}\cdot\text{min}^{-1} \times (-\log[\text{Fe}(\text{CN})_6^{3-}]/\text{M})$. For $[\text{Fe}(\text{CN})_6^{3-}] > 0.05 \text{ M}$: $v = 1.65 \text{ nm}\cdot\text{min}^{-1}$. The dotted lines are extrapolations of the linear regression lines to their intersection.

dependence was only found for a concentration of the oxidant of up to about 15 mM (at $[\text{PhS}_2\text{O}_2] = 0.5 \text{ M}$, Figure 8). At higher ferricyanide concentrations, no further increase of the etch rate was observed, which is indicative of the oxidation step no longer being etch-rate-determining under these conditions.

The thiosulfate- and benzenethiosulfonate-based baths also differed in the quality of the achieved etch results, with gold substrates bearing microcontact printed SAM patterns comprising down to micron-sized features (Figure 9). In the absence of further additives, both baths produced a large number of etch defects (pinholes) at all concentrations of the respective sulfur-containing ligand. Pinholes originate from molecular defects in the ODT SAM layer, which mainly result from impurities and grain boundaries in the SAM layer and the imperfect flatness of the gold layer. The SAM defects allow the components of the etchant to reach the substrate surface, causing poor etch protection at these sites. Half-saturation of the thiosulfate etchant with 1-octanol, which is known to induce a defect-healing effect, can greatly reduce the number of pinholes (see micrographs A and B in Figure 9).²⁴ Anticipating a similar effect, we repeated our etch experiments with 1-octanol added at half-saturation to the benzenethiosulfonate bath. Indeed, a strong reduction of the number of pinholes was observed (Figure 9D,E). The etch result was, nevertheless, inferior to that obtained with the octanol-modified thiosulfate bath (Figure 9B). To further improve the bath, 1-octanol was substituted with different alkanesulfonates, which have proven to be excellent defect-healing additives in an acidic silver alloy etchant.²⁵ Nevertheless, in the case of the benzenethiosulfonate bath the presence of alkanesulfonates did not reduce the number of pinholes compared to the additive-free gold etchant (not shown).

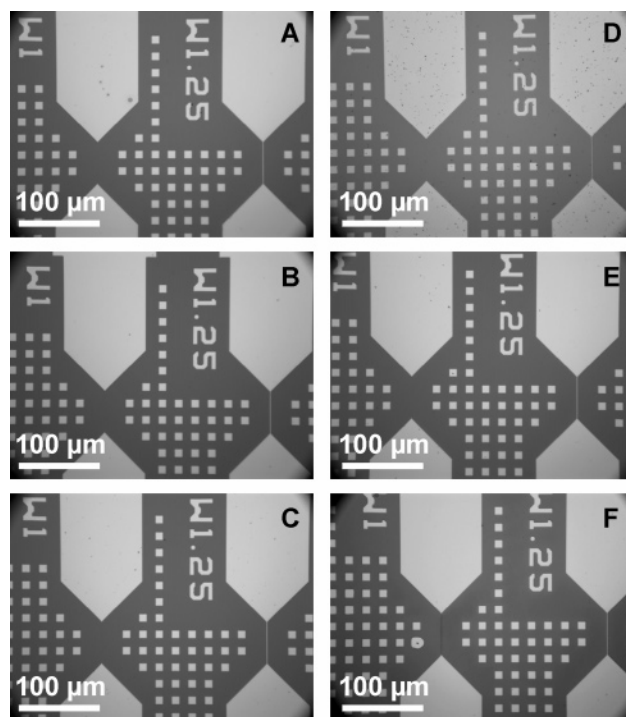


Figure 9. Optical micrographs of etched gold substrates ($20 \times 10 \text{ mm}^2$) that were microcontact printed with an ODT-inked PDMS stamp (15 s contact time) prior to etching. Bright areas correspond to elevated gold features. The used aqueous etchants had the following composition: $[\text{KOH}] = 1.0 \text{ M}$, $[\text{K}_3\text{Fe}(\text{CN})_6] = 0.01 \text{ M}$, $[\text{K}_4\text{Fe}(\text{CN})_6] = 0.001 \text{ M}$. The concentration of the thiosulf(on)ate was $[\text{Na}_2\text{S}_2\text{O}_3] = 0.1 \text{ M}$ (A–C) or $[\text{Na}(\text{PhS}_2\text{O}_2)] = 0.5 \text{ M}$ (D–F). No defect healing additive was added (A, D) or the solution was half-saturated with *n*-octanol (B, E) or DSA (C, F).

Assuming charge neutrality to be important for the effectiveness of the amphiphilic additive, we decided to test an alkanesulfonamide, 1-decanesulfonamide (DSA), as a possible additive. The saturation concentration of DSA in water at 25°C was determined to be $(4.0 \pm 0.5) \times 10^{-4} \text{ mol}\cdot\text{L}^{-1}$ by elemental analysis of the sulfur content of a saturated solution using inductively coupled plasma atomic emission spectrometry (ICP-AES). The solubility of DSA in a 1.0 M aqueous KOH solution was determined to be about 10 times higher $[(4.7 \pm 0.2) \times 10^{-3} \text{ mol}\cdot\text{L}^{-1}]$. DSA was therefore added to the basic benzenethiosulfonate bath at half-saturation. Upon etching microcontact printed gold substrates, the DSA-containing benzenethiosulfonate etchant yielded a better, essentially pinhole-free gold pattern (Figure 9F) than the bath containing 1-octanol (Figure 9E). For comparison, DSA was also used to replace 1-octanol in the thiosulfate etchant. In this case the etch results were essentially indistinguishable (Figure 9B,C); hence, DSA does not appear to offer a benefit over the much cheaper 1-octanol in this reference etchant.

The printed substrates that were developed with the thiosulfate–octanol and benzenethiosulfonate–DSA baths were further analyzed with atomic force microscopy (AFM). Figure 10 compares characteristic square (nominal size $10 \times 10 \mu\text{m}^2$) and line (nominal width $1.25 \mu\text{m}$) features of the etched gold layer as also depicted in Figure 9. Average widths of 9.55 ± 0.1 and $1.0 \pm 0.1 \mu\text{m}$, respectively, were measured for both substrates, indicative of the same small overetch of about 0.1 – $0.2 \mu\text{m}$ of both etchants. Considering

(24) Geissler, M.; Schmid, H.; Bietsch, A.; Michel, B.; Delamarche, E. *Langmuir* **2002**, *18*, 2374–2377.

(25) Burdinski, D.; Brans, H. J. A.; Decré, M. M. J. *J. Am. Chem. Soc.* **2005**, *127*, 10786–10787.

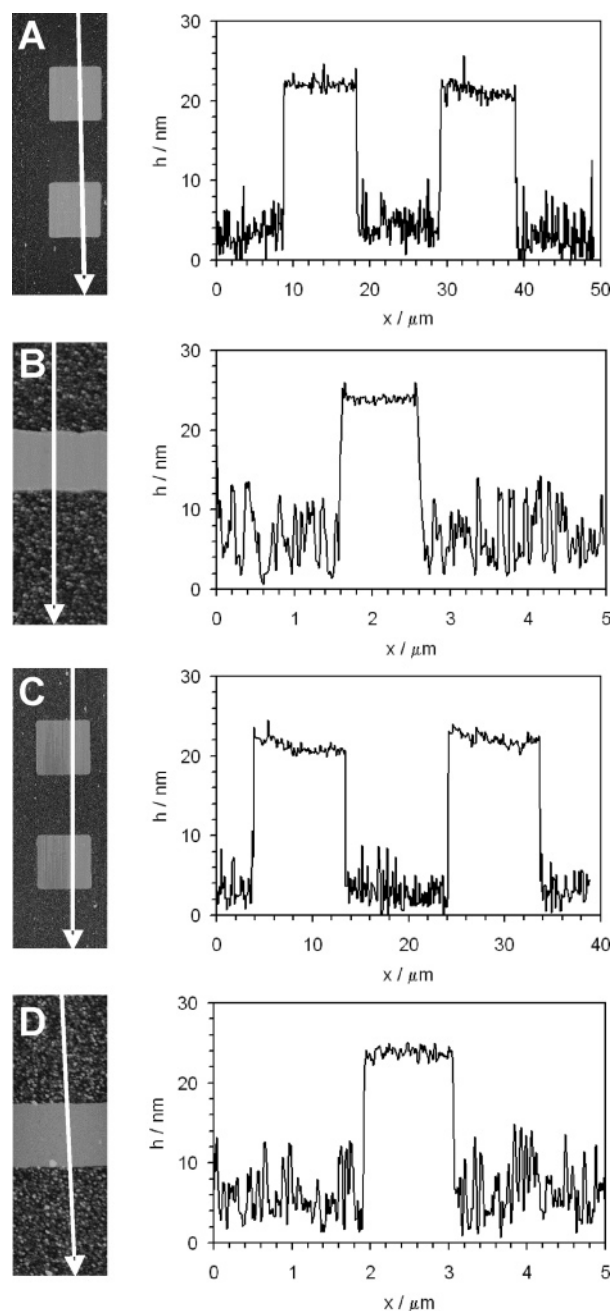


Figure 10. AFM results of the top gold layer on $20 \times 10 \text{ mm}^2$ silicon substrates that were microcontact printed with an ODT-inked PDMS stamp (15 s contact time) and etched with a thiosulfate or thiosulfonate etchant of the following composition: $[\text{KOH}] = 1.0 \text{ M}$, $[\text{K}_3\text{Fe}(\text{CN})_6] = 0.01 \text{ M}$, $[\text{K}_4\text{Fe}(\text{CN})_6] = 0.001 \text{ M}$. The concentration of the thiosulf(on)ate and the defect healing additive at half-saturation were $[\text{Na}_2\text{S}_2\text{O}_3] = 0.1 \text{ M}$ and n -octanol (A, B), or $[\text{Na}(\text{PhS}_2\text{O}_2)] = 0.5 \text{ M}$ and DSA (C, D). The analyzed features have nominal sizes of $10 \times 10 \mu\text{m}^2$ (squares in A and C) and $1.25 \mu\text{m}$ (lines in B and D). The roughness of the etched surfaces results from not completely removed gold particles or newly deposited debris.

that the final feature width is a combination of feature enlarging ink spreading during printing and the total overetch, which has just the opposite effect, several causes are imaginable for the slightly larger net overetch of the square compared to the line features. These include stamp deformation during printing,^{26–30} as well as feature-dependent and

inhomogeneous ink transfer.^{31–33} Their relative contribution depends significantly on the specific experimental setup. With respect to the overall pattern quality, the etch performance of the benzenethiosulfonate–DSA bath in terms of feature definition and pinhole formation was comparable to that of the thiosulfate–octanol bath.

We therefore decided to finally test the stability of the new and the reference etchant under ambient conditions in open containers. The decomposition process of the baths, which for better comparison did not contain the defect-healing additives in these particular experiments, was probed by using two independent methods. UV/vis spectroscopy was used to follow selectively changes in the concentration of the ferricyanide ion, which, being the only significantly colored species in these etchants, has a characteristic absorption band around 420 nm. At different time points after the respective stock solutions were mixed at time point zero of each experiment, samples were taken from the etchants, diluted (1:9) with deionized water, and analyzed. Figure 11 shows a plot of the absorbance measured at 420 nm against the time. In the case of the thiosulfate bath (panel A), the intensity of the 420 nm band decreased linearly to zero within less than 9 h, indicating a complete consumption of the ferricyanide ions. In the benzenethiosulfonate bath (panel B), the ferricyanide concentration changed less quickly, and even after 5 days, about 10% of the original absorbance at 420 nm was still detected. Here the absorbance decreased linearly in the beginning down to two-thirds of its original value within about 7 h, after which it further decreased exponentially with time. For both baths, experiments were performed under ambient light conditions as well as in the dark, and for none of them was observed a significant difference in the decomposition process (Figure 11).

As a second indicator, we studied the change of the etch performance of the baths over time by etching unpatterned gold substrates with aliquots taken from these baths at different time points. The average etch rates, as calculated from the total etch time, are plotted in Figure 11 for comparison with the in-parallel measured UV/vis data. For both etchants, the achieved etch rates decreased over time, and generally, they followed the same trend as described for the change of the ferricyanide concentration. This indicates a direct correlation of the consumption of the ferricyanide oxidant and the reduction of the etch power, which is in accordance with the above-described concentration-dependent etch studies and the general observation that the etch performance decreases with progressing decolorization of these etchants. Whereas the thiosulfate etchant became fully unreactive within less than 9 h, the benzene-

(26) Bietsch, A.; Michel, B. *J. Appl. Phys.* **2000**, *88*, 4310–4318.

(27) Decré, M. M. J.; Timmermans, P. H. M.; van der Sluis, O.; Schroeders, R. *Langmuir* **2005**, *21*, 7971–7978.

(28) Huang, Y. Y.; Zhou, W.; Hsia, K. J.; Menard, E.; Park, J.-U.; Rogers, J. A.; Alleyne, A. G. *Langmuir* **2005**, *21*, 8058–8068.

(29) Guo, Q.; Teng, X.; Yang, H. *Nano Lett.* **2004**, *4*, 1657–1662.

(30) Sharp, K. G.; Blackman, G. S.; Glassmaker, N. J.; Jagota, A.; Hui, C.-Y. *Langmuir* **2004**, *20*, 6430–6438.

(31) Sharpe, R. B. A.; Burdinski, D.; Huskens, J.; Zandvliet, H. J. W.; Reinhoudt, D. N.; Poelsema, B. *Langmuir* **2004**, *20*, 8646–8651.

(32) Delamarche, E.; Schmid, H.; Bietsch, A.; Larsen, N. B.; Rothuizen, H.; Michel, B.; Biebuyck, H. *J. Phys. Chem. B* **1998**, *102*, 3324–3334.

(33) Sharpe, R. B. A.; Titulaer, B. J. F.; Peeters, E.; Burdinski, D.; Huskens, J.; Zandvliet, H. J. W.; Reinhoudt, D. N.; Poelsema, B. *Nano Lett.* **2006**, *6*, 1235–1239.

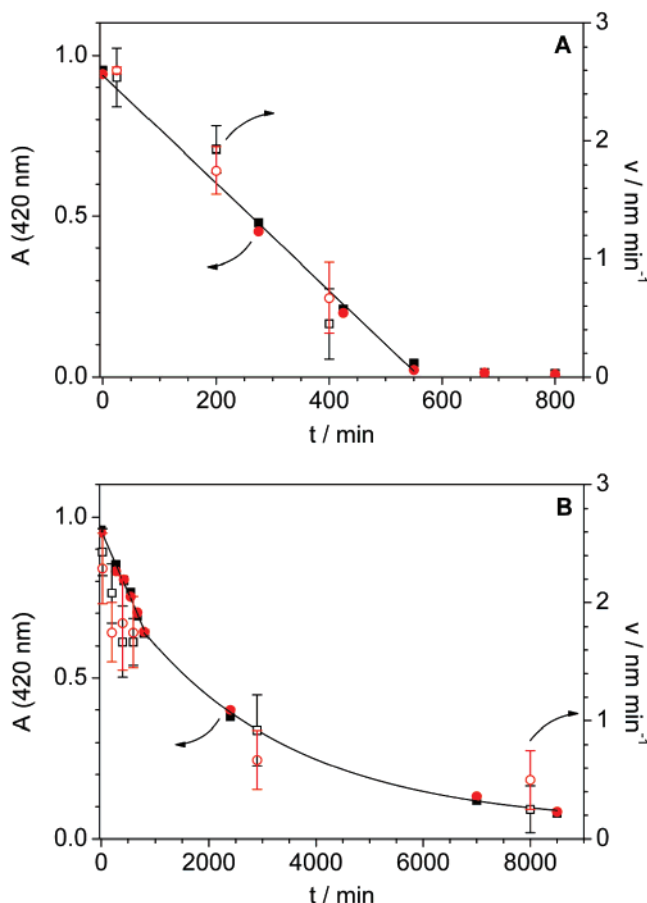
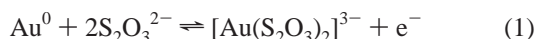


Figure 11. Absorbance at 420 nm (closed symbols, after 1:9 sample dilution with water, see Supporting Information for full spectra, Figure S1) as a function of time after mixing respective stock solutions for etch baths of the following composition: $[\text{KOH}] = 1.0 \text{ M}$, $[\text{K}_3\text{Fe}(\text{CN})_6] = 0.01 \text{ M}$, $[\text{K}_4\text{Fe}(\text{CN})_6] = 0.001 \text{ M}$, and different ligand concentrations of $[\text{Na}_2\text{S}_2\text{O}_3] = 0.05 \text{ M}$ (A) and $[\text{NaPhS}_2\text{O}_2] = 0.5 \text{ M}$ (B). Gold etch rates at different times after mixing of ligand and oxidant stock solutions (open symbols). The solutions were unprotected (red circles) or protected (black squares) from the laboratory light. Best fit of all absorbance data (1σ values in parenthesis): $A = 0.94(4) - 1.7(4) \times 10^{-3} \text{ min}^{-1} \times t$ (A); $A = 0.95(5) - 3.8(6) \times 10^{-4} \text{ min}^{-1} \times t$ (for $t < 800 \text{ min}$) and $A = 0.78(2) \exp(-3.4(2) \times 10^{-4} \text{ min}^{-1} \times t) + 0.04(2)$ (for $t > 800 \text{ min}$) (B).

thiosulfonate bath still showed some 20% of its original activity after more than 5 days.

Discussion

Thermodynamics and Kinetics of Gold Etching with Thiosulfate Solution. The etching of metallic gold is best described in terms of an electrochemical model that consists of coupled anodic and cathodic reactions. In thiosulfate solutions the overall anodic reaction as described in eq 1 has a standard reduction potential of 0.15 V.^{22,34}



The oxidatively formed gold(I) ion forms a linear, water-soluble bis(thiosulfate) complex.^{35,36} The gold ion is coor-

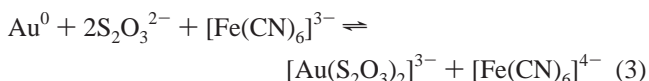
minated to the thiosulfate ligand via the sulfide-like terminal S atom, the electronic properties of which dominate the chemistry of the thiosulfate ion.^{22,37}

In the cathodic reaction ferricyanide is reduced to ferrocyanide with a standard reduction potential of 0.36 V.³⁸



Ferricyanide is a slightly less strong oxidant than dioxygen, which at pH 14 has a reduction potential of 0.40 V, but it has proven to be kinetically more effective in dissolving gold in alkaline thiosulfate solutions.¹¹

Although the overall etch reaction can formally be described as a combination of these two-half-reactions (eq 3), the actual etch mechanism is rather complicated.^{22,39,40}



It was, therefore, one aim of this study to find a simple description of the main factors that determine the practical gold dissolution rate under typical etching conditions.

For a standard thiosulfate–ferricyanide etch bath ($[\text{KOH}] = 1.0 \text{ M}$, $[\text{K}_2\text{S}_2\text{O}_3] = 0.1 \text{ M}$, $[\text{K}_3\text{Fe}(\text{CN})_6] = 0.01 \text{ M}$, $[\text{K}_4\text{Fe}(\text{CN})_6] = 0.001 \text{ M}$), we studied the progress of the gold dissolution by quenching the etch reaction at different time points and determining the thickness of the remaining gold layer by RBS analysis. The thickness of the gold layer decreased linearly with time at four temperatures between 5 and 35 °C without initial lag time. This means that under these conditions the observed time to clear (TTC, the time that is necessary to completely remove the unprotected gold layer from a wafer) can be directly translated to an average etch rate v ($v = d/\text{TTC}$, with d being the thickness of the gold layer). In this way, average etch rates were calculated in the subsequent experiments. The determined Arrhenius activation energy of $59 \pm 2 \text{ kJ}\cdot\text{mol}^{-1}$ is at the higher end of the range of activation energies ($25\text{--}60 \text{ kJ}\cdot\text{mol}^{-1}$) so far reported for gold dissolution in thiosulfate solutions.^{35,41} It can, therefore, be concluded that the reaction is chemically controlled, since diffusion controlled reactions usually have an activation energy of less than $25 \text{ kJ}\cdot\text{mol}^{-1}$.⁴² Chemically controlled etch reactions are generally favored, because the etch rate is independent of the position of the feature on the substrate surface, which can otherwise result in an edge effect or diffusion patterns, and it is not influenced by material transport processes, which would depend, for example, on the stirring rate.

In an earlier study, Xia et al. examined with a standard thiosulfate–ferricyanide gold etchant the dependence of the time to clear on the concentration of the main bath components.¹³ They found that the TTC decreased with an increase of the concentrations of thiosulfate and hydroxide,

(37) Ruben, H.; Zalkin, A.; Faltens, M. O.; Templeton, D. H. *Inorg. Chem.* **1974**, *13*, 1836–1839.

(38) Spiro, M.; Ravnö, A. B. *J. Chem. Soc.* **1965**, 78–96.

(39) Chandra, I.; Jeffrey, M. I. *Hydrometallurgy* **2004**, *73*, 305–312.

(40) Aylmore, M. G.; Muir, D. M. *Miner. Eng.* **2001**, *14*, 135–174.

(41) Breuer, P. L.; Jeffrey, M. I. *Miner. Eng.* **2000**, *13*, 1071–1081.

(42) Power, G. P.; Ritchie, I. M. In *Modern Aspects of Electrochemistry*; Plenum Press: London, 1975; Vol. 2, pp 199–250.

(34) Schmid, G. M.; Curley-Fiorino, M. E. In *Encyclopedia of Electrochemistry of the Elements*. Vol IV. Au, F, Po, S, Sb, Se, Sn, Te, Tl; Bard, A. J., Ed.; Marcel Dekker: New York, 1975; pp 87–178.

(35) Zhang, X. M.; Senanayake, G.; Nicol, M. J. *Hydrometallurgy* **2004**, *74*, 243–257.

(36) Perera, W. N.; Senanayake, G. *Inorg. Chem.* **2004**, *43*, 3048–3056.

but a kinetic effect of the ferricyanide concentration was not observed between 0.001 and 0.1 M. A conclusive, quantitative description of those experimental results was not provided.

We could confirm the general trends described for the dependence of the TTC on the thiosulfate and hydroxide ion concentration. In addition a similar dependence on the ferricyanide concentration was observed in sodium hydroxide solution. Plots of the calculated average etch rates against the respective ion concentrations allowed us to fit the experimental data with simple equations. It was found that the etch rate depended linearly on $\log[\text{S}_2\text{O}_3^{2-}]$ at a constant as well as a variable ionic strength. Similarly, it depended linearly on $\log[\text{OH}^-]$ at a constant ionic strength of 4.0 M in NaOH (NaClO_4) solution and showed an apparent broken reaction order of 0.5 in $[\text{OH}^-]$ under conditions of a variable ionic strength in KOH solution.

For the thiosulfate and hydroxide ion dependence at variable ionic strength, we also calculated the average etch rates from the TTC data reported by Xia et al., assuming a linear etch progress over time.¹³ With the exception of the data points for the highest etch rates, both of those data sets could be described excellently in the same way with a $\nu \sim \log[\text{S}_2\text{O}_3^{2-}]$ and a $\nu \sim [\text{OH}^-]^{1/2}$ fitting function, respectively. The small differences in the total etch rates between those data and the here reported results is not surprising, since it is known that the gold dissolution rate strongly depends on the microstructure of the gold film and hence on the particular gold deposition conditions.³⁹

In our experiments the etch rate increased linearly with $\log[\text{Fe}(\text{CN})_6^{3-}]$ between 0.001 and 0.1 M in sodium hydroxide solution, whereas Xia et al. reported the etch rate to be independent of the ferricyanide concentration in potassium hydroxide solution.¹³ This indicates an important role of the alkali cation in the etch mechanism. In sodium hydroxide solution the increase of the etch rate with increasing ferricyanide concentration was stronger under conditions of variable ionic strength than when the ionic strength was controlled at 4.0 M with balancing amounts of NaClO_4 . Studying the influence of the ionic strength on the etch rate, it was found that this could be described as $\nu \sim \log[\mu]$ in sodium hydroxide solution.

A linear dependence of reaction rates on the pH of the solution is not uncommon. A linear rate dependence on the logarithm of the concentration of other reaction partners, as seen here for the concentrations of thiosulfate and ferricyanide as well as the ionic strength, is less common. For homogeneous reactions this typically indicates the involvement of fast equilibria or the combined effect of a group of factors.⁴³ The observed positive dependence of the etch rate on the ionic strength is, nevertheless, not unexpected, since it implies that in the rate-determining step of the etch reaction components with a similar charge are involved. All the basic components of the etch bath, thiosulfate, ferricyanide, and hydroxide, are negatively charged. In strongly alkaline solution the gold surface carries a layer of adsorbed Au-

(OH)/ AuO^- , which is known to cause passivation against etching, among other reasons, due to the built up of a negative surface charge.^{8,44} In an early step of the dissolution reaction thiosulfate adsorbs at the gold surface, which in part substitutes surface-bound singly negative hydroxide groups with doubly negative thiosulfate ions.⁴⁵ This process is expected to be accelerated under high ionic strength conditions. In the presence of thiosulfate, surface passivation is further caused by a second mechanism, which involves the surface-catalyzed decomposition of thiosulfate and results in the formation of a negatively charged gold sulfide monolayer.^{35,40,46–48} The etch rate increase with increasing ionic strength therefore reflects most probably the mechanistic contribution of reactions between the negatively charge modified gold surface and anionic species of the etch solution, most prominently thiosulfate and ferricyanide.

In this context the influence of the type of alkali hydroxide can be understood. A linear dependence of the etch rate on the square root of the alkali hydroxide (MOH, M = Li, Na, K) concentration was observed for all three hydroxides under variable ionic strength conditions, while the etch rate was substantially higher (up to a factor of 2) for potassium than for both sodium and lithium hydroxide, at high MOH concentrations. The difference in base strength [$\text{p}K_b(\text{KOH}) = -2.25$, $\text{p}K_b(\text{NaOH}) = -0.7$, $\text{p}K_b(\text{LiOH}) = 0$]⁴⁹ can be safely assumed to be an important contributing factor. Zhang et al. suggest that the rate increase with pH can be attributed to the partial elimination of sulfur-like films from the gold surface in solutions with high concentrations of free hydroxide ions.⁴⁶ Nevertheless, the unusual concentration dependence ($\nu \sim \log([\text{KOH}] \text{ at } \mu = \text{const.})$) indicates a kinetic superposition with other factors. It has recently been reported that the presence of heavier inert cations, such as potassium, calcium, and cesium, enhances the oxidation of gold in thiosulfate-leaching solutions.³⁹ Two possible reasons for this observation have been discussed:^{39,45,50} (1) Cations, such as potassium, with a higher atomic mass are less hydrated compared to sodium and are, therefore, more likely to be adsorbed onto the gold surface. This can reduce the overall negative charge of the gold surface and facilitate the approach of negatively charged species. (2) The ion pair dissociation constants for the alkali metal ions with thiosulfate ions decrease in the sequence of $\text{Na} > \text{K} > \text{Rb} > \text{Cs}$. Therefore, one would expect K^+ to be more likely to form an ion pair with thiosulfate or gold thiosulfate than Na^+ . Ion pair formation stabilizes the intermediate and hence increases the etch rate. Both of these mechanistic proposals are supported by the found ionic strength dependence of the etch rate. It can also be expected that the cathodic reduction of ferricya-

(43) Wilkins, R. G. *Kinetics and Mechanism of Reactions of Transition Metal Complexes*, 2nd ed.; VCH: Weinheim, 1991.

(44) Sharpe, R. B. A.; Burdinski, D.; Huskens, J.; Zandvliet, H. J. W.; Reinhoudt, D. N.; Poelsema, B. *J. Am. Chem. Soc.* **2006**, *128*, 15560–15561.

(45) Senanayake, G. *Gold Bull.* **2005**, *38*, 170–179.

(46) Zhang, S.; Nicol, M. J. *J. Appl. Electrochem.* **2003**, *33*, 767–775.

(47) Lay, M. D.; Varazo, K.; Stickney, J. L. *Langmuir* **2003**, *19*, 8416–8427.

(48) Woods, R.; Hope, G. A.; Watling, K. M.; Jeffrey, M. I. *J. Electrochem. Soc.* **2006**, *153*, D105–D113.

(49) Perrin, D. D. *Ionisation constants of inorganic acids and bases in aqueous solution*, 2nd ed.; Pergamon Press: Oxford, 1982.

(50) Senanayake, G. *Hydrometallurgy* **2005**, *76*, 233–238.

nide is similarly catalyzed by the formation of a respective ion pair between alkali metal ions and the complex anion, a mechanism that has been shown before to be highly effective in potassium ion catalyzed outer-sphere electron-transfer reactions of ferricyanide.⁵¹

Kinetics of Gold Etching with Benzenethiosulfonate Solution. An important shortcoming of the thiosulfate–ferricyanide bath is its low stability, which stimulated us to consider thiosulfate derivatives that we expected to be less sensitive to oxidative decomposition as a substitute.

A (negative) ionic charge of the gold-complexing ligand appears to be important for a good selectivity of the etchant.⁵² Iodine–iodide as well as thiourea-based baths have been reported to be prone to pinhole formation, which indicates some tendency to penetrate a hydrophobic SAM. In both baths at least one of the reactive species is charge neutral and all of them are fairly lipophilic.

In the thiosulfate anion, one negative charge is partially located on the terminal sulfur atom, which serves as the donor atom for gold coordination.²² We expected that removal of the second, more delocalized negative charge would reduce the oxidation sensitivity of the molecule and stabilize the solution while causing only a small change of the etch performance. Benzenethiosulfonate, in which one negatively charged oxide group of thiosulfate is substituted with a phenyl group, is one of the compounds that we tested.

The new benzenethiosulfonate–ferricyanide bath indeed proved to be an efficient etchant. At ligand concentrations below 1.0 M, etch rates were, however, significantly lower for the thiosulfate bath, under otherwise identical conditions. This can be assumed to be a direct consequence of the lowering of the molecular charge. Whereas in the case of thiosulfate a linear dependence of the etch rate on the logarithm of the ligand concentration was found, the etching rate increased linearly with the concentration of benzenethiosulfonate. This indicates some change in the rate-determining step of the etch reaction. A practical consequence is that with the new ligand the etch rate can be controlled more effectively by changing the ligand concentration.

It is interesting to note that in recent electrochemical studies with thiosulfate solutions, substitution of potassium with ammonium ions has been reported to result in a substantial increase of the gold dissolution rate, and the use of ammonium thiosulfate in gold leaching solutions has therefore been recommended.^{39,46,50,53} Similarly the use of ammonium salts in benzenethiosulfonate–ferricyanide gold etch baths may result in an improved etch rate.

Above about 50 mM, increasing the ferricyanide concentration did not accelerate etching anymore ($[\text{PhS}_2\text{O}_2^-] = 0.5 \text{ M}$, $[\text{KOH}] = 1.0 \text{ M}$), whereas at lower, more typical concentrations ($[\text{Fe}(\text{CN})_6^{3-}] = 10 \text{ mM}$, $[\text{Fe}(\text{CN})_6^{4-}] = 1 \text{ mM}$) the etch rate increased linearly with the logarithm of the ferricyanide concentration. The same rate dependence was observed for the thiosulfate bath in sodium hydroxide solution.

With both baths the formation of a significant number of etch defects was observed, with the benzenethiosulfonate bath even more than with the reference bath. These are ascribed to molecular defects in the ODT layer, which result from impurities and the imperfect flatness of the substrate surface. Half-saturation of the thiosulfate etchant with 1-octanol is known to induce a defect-healing effect in neutral and alkaline etching solutions due to the formation of a SAM-stabilizing ad-layer.^{24,54} In the case of the benzenethiosulfonate bath, addition of 1-octanol also reduced the defect density, but the effect was insufficient to achieve the same etch quality as with the reference bath. The more lipophilic benzenethiosulfonate molecule has a higher tendency to penetrate such defect sites, which results in a more pronounced defect formation.

As an alternative additive bearing a longer alkyl chain, a decanesulfonate had been used successfully in strongly acidic solutions, in which it becomes charge-neutral due to protonation, but it turned out to be ineffective in the present alkaline solutions due to complete deprotonation.²⁵ Guided by the assumption that charge neutrality and a longer alkyl chain are important for the effectiveness of the amphiphilic additive, we found 1-decanesulfonamide (DSA) to be sufficiently active in this function. Depending on the pH, DSA is about 10^2 – 10^3 times more soluble in water than 1-octanol [$c_{\text{sat}}(\text{octanol}) = 4.1 \times 10^{-6} \text{ M}^{55}$], so that at half-saturation a concentration ($\sim 2 \times 10^{-3} \text{ M}$) was used successfully that is similar to the one described to be the optimum for the decanesulfonate additive ($\sim 10^{-3} \text{ M}$) in acidic solution.²⁵ In the presence of the respective additive, the thiosulfate–octanol and the benzenethiosulfonate–DSA bath both caused a similar gold overetch of about 0.1–0.2 μm at the same low defect level; hence, they performed comparably in terms of feature definition and defect formation.

Etch Bath Stability. In addition to the etch rate and quality, the stability of an etchant is the third key process parameter. Etchants based on sulfur-containing compounds, such as thiourea and thiosulfate, are particularly sensitive to oxidative decomposition. The degradation process is chemically complex and in the case of thiosulfate not completely understood. It is known that sulfate, which is a thermodynamically stable degradation product, and trithionate and tetrathionate, which are metastable degradation products, are commonly present in thiosulfate etch solutions, but the factors influencing the formation and interaction of these species are not clear. While tetrathionate is an important initial thiosulfate oxidation product, it is unstable under alkaline conditions.^{40,56} Although earlier kinetic studies have revealed some details of the controlled reaction between thiosulfate and ferricyanide, which forms the main path of the thiosulfate decomposition reaction, we were interested in an assessment of

(51) Zahl, A.; van Eldik, R.; Swaddle, T. W. *Inorg. Chem.* **2002**, *41*, 757–764.

(52) Schoenfish, M. H.; Pemberton, J. E. *Langmuir* **1999**, *15*, 509–517.

(53) Senanayake, G. *Hydrometallurgy* **2005**, *77*, 287–293.

(54) French, M.; Creager, S. E. *Langmuir* **1998**, *14*, 2129–2133.

(55) Riddick, J. A.; Bunger, W. B.; Sakano, T. K. *Organic Solvents*, 4th ed.; *Techniques of Chemistry*; Vol. II; Weissberger, A., Ed.; John Wiley & Sons: New York, 1986.

(56) Ahern, N.; Dreisinger, D.; van Weert, G. *Can. Metal. Quart.* **2006**, *45*, 135–144.

the lifetime of the above etchants under practical, ambient conditions.^{57–59}

The above experiments allowed us to define two etching solutions with $[\text{S}_2\text{O}_3^{2-}] = 0.05 \text{ M}$ or $[\text{PhS}_2\text{O}_2^-] = 0.5 \text{ M}$ and identical concentrations of the other bath components to show a similar etch rate of about $2 \text{ nm}\cdot\text{min}^{-1}$. These two solutions were selected to study their stability. In our experiments, thiosulfate and benzenethiosulfonate were present in excess of the oxidant ferricyanide, the concentration of which could easily be followed spectrophotometrically to probe the decomposition process. Furthermore, in both baths the reduction of ferricyanide to ferrocyanide was found to coincide with a gradual decrease of the gold etch rate. Using these two indicators, we determined the benzenethiosulfonate bath to be still active after 5 days, while the thiosulfate bath was fully decomposed within less than 9 h. This translates to an appreciable 15-times higher bath stability of the benzenethiosulfonate etchant. In both cases, the decomposition process was not influenced by the presence of ambient light, which was noted before for the thiosulfate etchant.¹³

Ferricyanide consumption in the thiosulfate etchant was found to proceed linearly in time over the entire decomposition process, which is indicative of a zero-order process with respect the iron complex, in accordance with literature data.^{57,58} In the benzenethiosulfonate bath, the first phase of the decomposition process showed similar ferricyanide-independent kinetics, but thereafter the process became dominated by a ferricyanide-dependent reaction. Avoiding further speculations about the details of this process, we interpret these results in terms of a nontrivial multistep reaction chain that may involve benzenethiosulfonate-based association and disproportionation equilibria similar to the ones postulated for the thiosulfate case.^{57,58}

Since all reaction solutions were open to the air, oxygen may have accelerated bath decomposition. This specific reaction has, however, been reported to be relatively slow, despite its comparably high thermodynamic driving force.^{35,38} Nevertheless, the thiosulfate bath could hardly be used reliably for longer than an hour after preparation and its overall stability was lower than expected on the basis of literature reports.^{57–59} It is known that several factors can accelerate the reaction between thiosulfate and ferricyanide. These include catalytic amounts of transition metals, very high base concentrations, and high concentrations of ammonium or potassium ions, at least the latter two of which may contribute here.^{38,45,56} It has been proposed that, similar to the acceleration of the gold dissolution reaction, the thiosulfate decomposition is catalyzed by the formation of ion pairs between the negative reactants and these cations.^{56,57} In accordance with literature results on the catalysis of thiosulfate decomposition by noble metal surfaces, we have further observed a significantly faster decomposition of thiosulfate as well as benzenethiosulfate baths that were

actually used in gold etching reaction, considering that the amount of reagents consumed due to the actual etching was negligible.^{38,60–62}

A number of options exist for the further improvement of the above etchant. Charged and uncharged substituents can be introduced most easily in the para-position of the aromatic benzenethiosulfonate ring, which would allow for a fine-tuning of the gold binding interaction and the oxidation sensitivity. Addition of ammonia or ammonia–thiourea has been reported to further accelerate gold dissolution, but as discussed above, this may be associated with a faster bath decomposition.^{39,50,53} The latter effect could potentially be countered by using ferric oxalate as the oxidant, which reportedly forms a more stable thiosulfate etch bath that, nevertheless, cannot be strongly alkaline due to fast iron oxide formation.⁶³ Finally, the new etchant needs to be tested with other SAM resists. In particular, carboxylate-terminated SAMs may in alkaline solution provide a better resistance against the less hydrophobic, anionic benzenethiosulfonate ligand than CH_3 -terminated SAMs.^{11,23}

Conclusions

Gold dissolution in a standard thiosulfate–ferricyanide etch solution is a complicated process. Etch-rate-determining under most conditions are the concentrations of thiosulfate, ferricyanide, and hydroxide, for which a logarithmic concentration dependence was observed. A high ionic strength and potassium ions catalyze gold dissolution most probably due to the formation of potassium–reagent ion pairs, which reduce the Coulomb repulsion between the negatively charged reaction partners. The thiosulfate–ferricyanide etchant is intrinsically unstable. On the basis of the observed reduction of the oxidant ferricyanide and the decrease of the average etch rate over time, the bath was found to decompose within several hours. The contact with a gold surface in an actual etch process further catalyzed the decomposition. The gold ligand thiosulfate was therefore substituted with benzenethiosulfonate, which was expected to be less oxidation sensitive due to its lower negative charge. The benzenethiosulfonate–ferricyanide bath decomposed in the course of days instead of several hours. Since its etch efficiency was also reduced, it was necessary to use a significantly higher concentration of the gold ligand to achieve a sufficiently high etch rate. The gold etch quality of the new bath was also lower, but the number of etch defects could be reduced by the addition a new defect healing additive, 1-decanesulfonamide, which was found to be more effective than 1-octanol in this new etch solution. The etch rate of the benzenethiosulfonate-based bath may be further increased by introducing suitable substituents at the aromatic ring of the ligand in combination with the use of catalytically active additives in the etchant.

(57) Howlett, K. E.; Wedzicha, B. L. *Inorg. Chim. Acta* **1976**, *18*, 133–138.

(58) Panda, R. K.; Neogi, G.; Ramaswamy, D. *Bull. Soc. Chim. Belg.* **1981**, *90*, 1005–1016.

(59) Dasgupta, G.; Mahanti, M. K. *Afinidad* **1985**, *42*, 506–508.

(60) Freund, P. L.; Spiro, M. J. *Phys. Chem.* **1985**, *89*, 1074–1077.

(61) Li, Y.; Petroski, J.; El-Sayed, M. A. *J. Phys. Chem. B* **2000**, *104*, 10956–10959.

(62) Sharma, R. K.; Sharma, P.; Maitra, A. *J. Colloid Interface Sci.* **2003**, *265*, 134–140.

(63) Chandra, I.; Jeffrey, M. I. *Hydrometallurgy* **2005**, *77*, 191–201.

Acknowledgment. We thank our colleagues Harry A. G. Nulens for AFM analyses, J. H. M. Snijders for RBS measurements, T. Haex and J. Smulders for ICP-AES analyses, as well as Patrick P. J. van Eerd and Michel M. J. Decré for experimental and general support.

Supporting Information Available: UV–vis spectra measured during decomposition studies of etch baths (Figure S1). This material is available free of charge via the Internet at <http://pubs.acs.org>.

CM070864K